Analysis of Influencing Factors on Material Removal Rate in External Cylindrical CBN Grinding of HARDOX 500 Steel

LE HOANG ANH[1], TRAN HUU DANH[1], VO THANH TUAN[2], DINH VAN THANH[3], NGUYEN MANH CUONG[4,*]

[1]Vinh Long University of Technology Education,
73 Nguyen Hue Street, Vinh Long City 85100,
VIETNAM

[2]Long An College,
Long An Ward, Tay Ninh Province 840000,
VIETNAM

[3]East Asia University of Technology,
Trinh Van Bo Street, Hanoi City 12000,
VIETNAM

[4]Thai Nguyen University of Technology,
3/2 street, Tich Luong ward, Thai Nguyen City 251750,
VIETNAM

**Corresponding Author*

Abstract: - This paper presents an investigation into the influence of grinding parameters on the material removal rate (MRR) during external cylindrical grinding of HARDOX 500 steel using a CBN grinding wheel. A quadratic response surface methodology (RSM) model was established to examine the individual, interaction, and quadratic effects of depth of cut, spindle speed, and feed rate on MRR. The experimental data were evaluated by analysis of variance (ANOVA) together with effect size analysis. The results indicate that depth of cut, its interaction with feed rate, and the quadratic term of depth of cut are the most influential factors affecting MRR ($p < 0.01$), whereas the influence of spindle speed is insignificant within the investigated range. The developed model predicts MRR with high accuracy ($R^2 = 0.9998$) and can be used as a practical tool for selecting suitable grinding parameters to improve machining productivity.

Key-Words: - Material removal rate; External cylindrical grinding; CBN grinding wheel; HARDOX 500 steel; Response surface methodology; ANOVA; Effect size; Process optimization.

Received: April 4, 2026. Revised: August 7, 2026. Accepted: September 4, 2026. Available online: November 27, 2026.

1 Introduction

Cubic boron nitride (CBN) grinding is widely used for machining hard-to-cut materials due to its high thermal conductivity, excellent wear resistance, and ability to maintain sharp cutting edges under severe grinding conditions. In recent years, many studies have focused on improving the performance of CBN grinding wheels by optimizing wheel structure, bond materials, and grinding parameters to enhance wear resistance and material removal capability, [1], [2], [3].

In addition, surface structuring and the use of polycrystalline CBN abrasives have been reported to improve grinding stability and surface quality under demanding machining conditions, [1], [2]. Predictive wear models for electroplated CBN tools have also been developed, enabling accurate estimation of tool life under various loading regimes, [3]. In addition, in-situ monitoring techniques based on wireless sensing have demonstrated potential for improving process stability and control in precision grinding applications, [4].

The wear behavior of electroplated CBN wheels has been shown to be strongly influenced by grinding parameters, while optimized wheel geometries have resulted in improved grindability

for high-performance alloys, [5], [6]. Analytical and empirical models were also used to explain the material removal mechanism in CBN grinding, which gives a theoretical basis for predicting the material removal rate (MRR), [7]. Other studies showed that the change of wheel topography, the pore structure and the bond type have a clear effect on grinding forces, thermal and mechanical loads, and surface integrity when grinding difficult-to-cut materials, [8], [9], [10], [11], [12].

In [13] and [14], authors studied the micro-fracture of CBN grains and developed new vitrified bond wheels. Their results showed that the grinding efficiency, tool life and surface finish were improved considerably. These studies have helped to better understand the fabrication of CBN wheels, their wear mechanisms and the ways to improve the grinding process. However, most of them were carried out on aerospace alloys, bearing steels or cermets.

For ultra-high-strength steels such as HARDOX 500, the number of studies on external cylindrical grinding with CBN wheels is still small. In particular, the effect of grinding parameters on MRR has not been evaluated quantitatively. MRR is an important indicator of grinding productivity. However, only a few studies have used statistical tools, such as response surface methodology (RSM) and analysis of variance (ANOVA), to determine how much each grinding parameter and their interactions affect MRR for this material.

Therefore, in this study, a quadratic RSM model is used to analyze the factors affecting MRR in external cylindrical CBN grinding of HARDOX 500 steel. The effects of depth of cut, spindle speed, and feed rate, together with their interaction and quadratic terms, are evaluated through ANOVA and effect size analysis. This approach not only identifies the dominant factors governing MRR but also provides a reliable predictive framework for parameter optimization aimed at improving grinding productivity.

2 Experimental Work

Experiments were carried out on a CNC milling machine to evaluate the effect of the input parameters on the material removal rate (MRR) in CBN grinding. Figure 1 shows the experimental setup, which includes a CNC milling machine (Model M-V50C, Japan), a CBN grinding wheel with a diameter of 125 mm, and HARDOX 500 steel workpieces. During grinding, the depth of cut (a□), the feed rate (f) and the spindle speed (n) are controlled at the same time. These three parameters directly decide the contact condition between the CBN wheel and the workpiece.

In this study, three input parameters were investigated: depth of cut a_p (mm), feed rate f (mm/min) and spindle speed n (rev/min). The experiments were designed according to the Box–Behnken design (BBD) with 15 runs. With this design, both the main effects and the interaction effects can be estimated, while the number of experiments is smaller than that of a full factorial design.

The ranges of depth of cut (a_p = 0.01–0.03 mm), spindle speed (n = 4000–5000 rpm) and feed rate (f = 2000–3000 mm/min) were chosen based on the capability of the machine tool, the recommendations of the CBN wheel manufacturer and the results of some trial experiments. The trial experiments were done to avoid unstable grinding conditions such as chatter, wheel loading or thermal damage. Thus, all experimental runs were carried out under stable and repeatable conditions.

MRR was determined by the gravimetric method. This method is often used in EDM and grinding research because it gives accurate and repeatable results. Before each test, the workpiece was cleaned with ethanol, dried with warm air and weighed on an analytical balance with a resolution of 0.1 mg. After grinding, the workpiece was cleaned and dried in the same way and then weighed again.

The material removal rate (g/min) was calculated according to Eq. (1):

$$MRR = \frac{m_{before} - m_{after}}{t} \cdot 60 \qquad (1)$$

where m_{before} and m_{after} are workpiece masses before and after machining (g) and t is machining time (s).

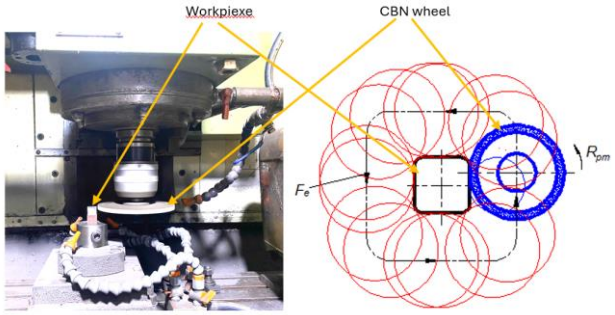

Fig. 1: Experimental setup for external cylindrical CBN grinding of HARDOX 500 steel, illustrating the CBN grinding wheel, workpiece, and the main input parameters: depth of cut (a_p), feed rate (f), and spindle speed (n).
Source: created by the authors

The experimental plan and the measured MRR values are summarized in Table 1. These data served as the basis for subsequent statistical modeling and analysis using response surface methodology (RSM) and analysis of variance (ANOVA).

Table 1. Input factors and output results

No.	a_p (mm)	n (rpm)	f (mm/min)	MRR (g/min)
1	0.01	4000	2500	0.127
2	0.03	4000	2500	0.378
3	0.01	5000	2500	0.127
4	0.03	5000	2500	0.378
5	0.01	4500	2000	0.102
6	0.03	4500	2000	0.305
7	0.01	4500	3000	0.152
8	0.03	4500	3000	0.454
9	0.02	4000	2000	0.191
10	0.02	5000	2000	0.191
11	0.02	4000	3000	0.284
12	0.02	5000	3000	0.284
13	0.02	4500	2500	0.237
14	0.02	4500	2500	0.237
15	0.02	4500	2500	0.237

Source: created by the authors

3 Results and Discussion

3.1 Model Adequacy and Statistical Overview

The quadratic RSM analysis on the CBN grinding dataset for HARDOX 500 demonstrated excellent agreement between the predicted and experimental MRR values (g/min). The statistical summary shows: n = 15, RMSE = 0.002276 g/min, R^2 = 0.999826 (adjusted R^2 = 0.999513), and a global F-test for the null hypothesis "all coefficients except the intercept are zero" yielding F(9,5) = 3191.37; p = 7.44×10^{-9}, confirming the very high statistical significance of the model.

The adequacy of the developed quadratic RSM model was evaluated using standard statistical indicators, as summarized in Table 2.

Table 2. Summary of the RSM model adequacy for MRR (g/min)

Metric	Value
Number of observations	15
RMSE (g/min)	0.002276
R^2	0.999826
Adjusted R^2	0.999513
Global F-test (d_f = 9,5)	3191.37 (p = 7.44×10^{-9})

Source: created by the authors

3.2 Stability and Error Analysis

To evaluate the stability and reliability of the grinding experiments, measurement uncertainty and model adequacy were examined. The material removal rate (MRR) was determined using a gravimetric method with an analytical balance of 0.1 mg resolution, and machining time was recorded using a digital timer. The combined measurement uncertainty was estimated through error propagation and was found to be significantly smaller than the observed variations in MRR caused by changes in grinding parameters, indicating that the experimental results are reliable.

In addition, residual diagnostics were performed to assess the adequacy of the developed quadratic RSM model. The diagnostics included checks for normality, constant variance, and independence of residuals. The results indicated no severe violations of regression assumptions, suggesting that the developed model provides a statistically sound and stable representation of the grinding process within the investigated design space.

3.3 Effect of Technological Parameters on MRR

Depth of cut (a_p) is the dominant factor, showing a strong positive non-linear effect within the studied range: a large positive quadratic term (a_p^2 = 154.81, p ≈ 4.7×10^{-5}) and a highly significant positive interaction with feed rate ($a_p\times f$ = 0.004911, p ≈ 4.0×10^{-6}).

Feed rate (f) shows no significant main effect (p ≈ 0.854), but amplifies MRR through its interaction with a_p, indicating that the benefit of increasing f becomes evident when a_p is also increased.

Spindle speed (n) exhibits no statistically significant influence within the experimental range (p ≈ 0.742), and higher-order or interaction terms involving n are also insignificant. This suggests low sensitivity of MRR to n in the tested range of 4000–5000 rpm.

From a physical perspective, the dominant influence of depth of cut (a_p) on MRR is expected, as increasing a_p enlarges the instantaneous material engagement zone, thereby increasing the removed material volume per unit time. The significant positive interaction between a_p and f indicates that higher feed rates become effective only when sufficient material engagement is ensured by a larger depth of cut. Meanwhile, spindle speed (n) mainly changes the cutting speed and the heat in the grinding zone. Therefore, its effect on MRR is very small in the studied range.

The same trends can be seen in Figure 2 and Figure 3.

In Figure 2 (effect barplot of the standardized parameters), a_p has the largest absolute effect, followed by f, while the effect of n is close to zero.

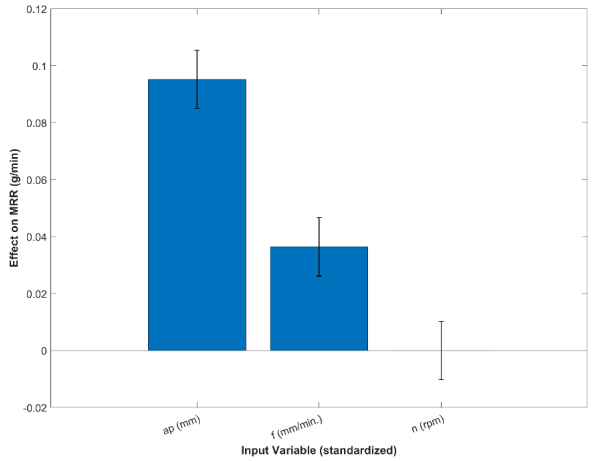

Fig. 2: Standardized effects of the input parameters on MRR (g/min)
Source: created by the authors

Figure 2 confirms that a_p has the strongest standardized effect on MRR, whereas n contributes very little within the tested range. Physically, this is expected because increasing a_p directly enlarges the wheel–workpiece engagement cross-section and therefore increases the material volume removed per unit time. This result agrees with the ANOVA results, in which the quadratic term a_p^2 and the interaction term $a_p \times f$ are highly significant ($p < 0.01$), while n is not significant ($p > 0.7$).

The main-effect plots in Figure 3 show that MRR increases almost linearly with a_p, increases slightly with f, and changes very little with n.

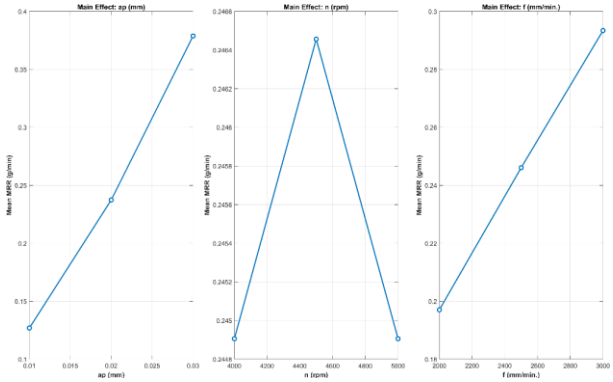

Fig. 3: Main effects of a_p, n and f on MRR (g/min)
Source: created by the authors

As seen in Figure 3, MRR increases strongly with depth of cut a_p, increases slightly with feed rate f, and is almost unchanged when spindle speed n changes. When a_p increases, the penetration depth and the contact area between the wheel and the workpiece become larger, so more material is removed per unit time. That is why MRR increases nearly linearly with a_p. The small effect of n shows that, in the range of 4000–5000 rpm, MRR depends mainly on the wheel–workpiece engagement, not on the spindle speed. This behavior agrees with the model terms, where a_p^2 and $a_p \times f$ are significant, while n is not.

3.4 Response Surface and Interaction Analysis

The a_p–n response surface at the median f (Figure 4) is almost flat along the n axis but slopes steeply along the a_p axis, reflecting the dominant influence of a_p and the low sensitivity to n. This agrees with the statistical results showing that n, n^2, and n×f are not significant.

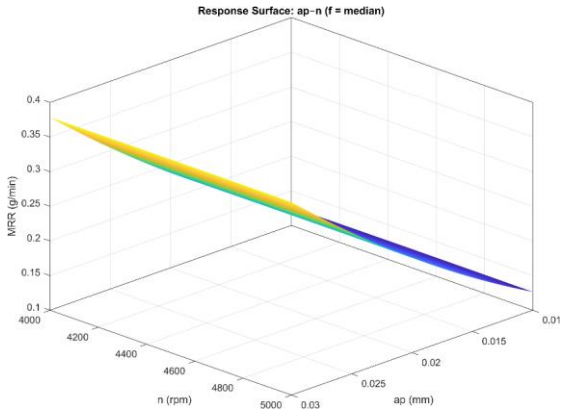

Fig. 4: Response surface of MRR as a function of a_p and n (f fixed at median)
Source: created by the authors

In Figure 4, the response surface is steep along the a_p axis but nearly flat along the n axis, indicating that MRR is mainly controlled by engagement (depth of cut) rather than spindle speed in the investigated region. From a physical standpoint, changing n within 4000–5000 rpm primarily modifies cutting speed and thermal conditions, but it does not substantially change the instantaneous material engagement volume, which explains the weak effect on MRR. The statistical results also confirm this, since n and its quadratic and interaction terms are not significant.

Figure 5 shows the contour plot of MRR versus a_p and f, with n kept at its median value. The contour lines are nearly parallel to the f axis and change clearly along the a_p axis. When a_p increases, the effect of f on MRR becomes larger, which reflects the significant positive interaction $a_p \times f$. The shape of the contour lines also shows the strong

non-linear effect of a_p and the combined effect of a_p and f on MRR.

3.5 Technological Implications and Limitations

To maximize MRR within the studied range, both a_p and f should be increased simultaneously, taking into account real-world constraints such as power, wheel wear, and surface finish requirements, which were not modeled in this study. Adjusting n within the range of 4000–5000 rpm has little effect on MRR. These conclusions are supported by both the statistical analysis and the graphical evidence above.

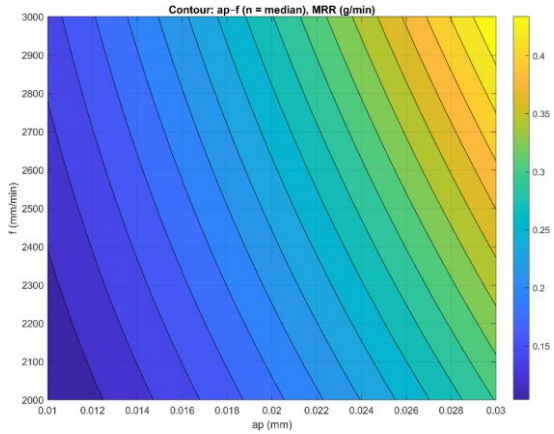

Fig. 5: Contour plot of MRR as a function of a_p and f (n fixed at median)
Source: created by the authors

Table 3. Key estimated coefficients from the RSM model for MRR (g/min)

Term	Estimate (±SE)	p-value	Interpretation
a_p	−5.8779 ± 1.2662	0.00562	Negative linear term but outweighed by positive a_p^2 and $a_p \times f \rightarrow$ net increase with a_p.
a_p^2	+154.8090 ± 11.8426	$4.67\times10^{-}$ p	Strong positive curvature effect of a_p.
$a_p \times f$	+0.004911 ± 0.000228	$3.96\times10^{-}$ p	Highly significant positive interaction: higher f amplifies a_p's effect.
f	-6.0×10^{-6} ± 3.2×10^{-5}	0.8538	Not significant when considered alone.
n	$+1.5\times10^{-5}$ ± 4.4×10^{-5}	0.7417	Not significant; low sensitivity within 4000–5000 rpm.

Source: created by the authors

It can be seen from Figure 5 that the effect of feed rate f on MRR becomes stronger at a larger depth of cut a_p. When a_p is small, the wheel only removes a thin layer, so increasing f does not increase the removed mass per unit time much. When a_p is large, a higher f allows more material to pass through the grinding zone, and MRR increases clearly. This supports the significant positive interaction term $a_p \times f$ reported in the RSM model (Table 3).

4 Conclusion

In this study, a quadratic RSM model was used to analyze the effects of depth of cut (a_p), spindle speed (n) and feed rate (f) on MRR in CBN grinding of HARDOX 500 steel. The main conclusions are as follows:

1. Prediction accuracy: The quadratic RSM model fits the experimental data very well, with R^2 = 0.999826 and RMSE = 0.002276 g/min. The global F-test is highly significant ($p < 10^{-8}$). Therefore, the model can be used to predict MRR with high reliability.
2. Effect of depth of cut: Among the three parameters, a_p has the largest effect on MRR. Both the quadratic term of a_p and its interaction with f are positive and significant. This means that MRR increases strongly when a_p increases, especially when f is also increased.
3. Interaction effect: The main effect of f alone is not significant. However, the interaction between f and a_p is positive and highly significant. Thus, increasing a_p and f at the same time gives a higher MRR.
4. Effect of spindle speed: In the range of 4000–5000 rpm, n has very little effect on MRR. Therefore, n can be adjusted to meet other process requirements, such as temperature, vibration or tool wear, without a large change in MRR.
5. Practical application: To obtain a high MRR in the studied range, a_p and f should be increased together. However, the machine power, wheel wear and surface quality must also be considered, because these factors were not included in the model.

Declaration of Generative AI and AI-assisted Technologies in the Writing Process

During the preparation of this work, the author(s) utilized artificial intelligence (AI) technologies solely for the purpose of linguistic refinement and grammatical correction. Following the application of these tools, the author(s) comprehensively reviewed, verified, and edited the resulting text. The author(s) maintain full accountability and responsibility for the accuracy, integrity, and final content of the publication.

References:

[1] Z. Wang, J. Li, Q. Liu, L. Chen, J. Lv, T. Yu, and J. Zhao, No-impact trajectory design and fabrication of surface structured CBN grinding wheel by laser cladding remelting method, Optics & Laser Technology, Vol. 181, no. C, 2025, Art. no. 111956. https://doi.org/10.1016/j.optlastec.2024.111956

[2] P. Breuer, T. Künkel, J. Werner, U. Müller, T. Bergs, and T. E. Weirich, Investigation of the structural stability of polycrystalline cBN under near-industrial grinding process conditions, *International Journal of Refractory Metals and Hard Materials*, Vol. 122, 2024, Art. no. 106720. https://doi.org/10.1016/j.ijrmhm.2024.106720

[3] H. Jamshidi, A. Bagherzadeh, E. Budak, and H. Ghadbeigi, A predictive wear model in grinding using single-layer electroplated cBN tools, *Journal of Manufacturing Processes*, Vol. 127, 2024, pp. 251-258. https://doi.org/10.1016/j.jmapro.2024.07.121

[4] L. Hu, L. H. Pueh, Z. Wang, and Y. Wang, Surface performance control and evaluation of precision bearing raceway with wireless sensing CBN grinding wheel, *Wear*, Vol. 568-569, 2025, Art. no. 205966. https://doi.org/10.1016/j.wear.2025.205966

[5] B. Kirsch, Quantitative analysis of the wear of electroplated cBN grinding wheels when grinding AISI 4140, Wear, 2025, Volumes 578–579, Art. no. 206227. https://doi.org/10.1016/j.wear.2025.206227

[6] Benkai LI, Wenfeng Ding, YeJun Zhu, Changhe Li, Yanbin Zhang, Min Yang, Xiao Ma, Mingzheng Liu, Xin Cui, Design and grindability assessment with cup shaped electroplated CBN wheel grinding turbine disc slots of powder metallurgy superalloy FGH96, Chinese Journal of Aeronautics, vol. 37, no. 9, 2024, pp. 521-534. https://doi.org/10.1016/j.cja.2023.12.030

[7] M. Deja, The use of Preston equation to determine material removal during lap-grinding with electroplated CBN tools, *Wear*, vol. 528-529, 2023, Art. no. 204968. https://doi.org/10.1016/j.wear.2023.204968

[8] M. Bredthauer, P. Snellings, P. Mattfeld, and T. Bergs, Wear-related topography changes for electroplated cBN grinding wheels and their effect on thermo-mechanical load, *Wear*, vol. 512-513, 2023, Art. no. 204543. https://doi.org/10.1016/j.wear.2022.204543

[9] B. Zhao, W. Ding, G. Xiao, J. Zhao, and Z. Li, Effects of open pores on grinding performance of porous metal-bonded aggregated cBN wheels during grinding Ti–6Al–4V alloys, *Ceramics International*, vol. 47, no. 22, 2021, pp. 31311-31318. https://doi.org/10.1016/j.ceramint.2021.08.004

[10] B. Guo, Q. Meng, G. Wu, Q. Zhao, and S. Li, Parallel axis precision grinding of micro-tooth internal thread with the coarse-grains CBN wheels, *Journal of Manufacturing Processes*, vol. 74, 2022, pp. 474-485. https://doi.org/10.1016/j.jmapro.2021.12.042

[11] X. Chen, Y. Liang, Zhengyu Sun, Yu Zhao, Zhelun Ma, L. Chen, T. Yu, and J. Zhao, Grinding performance oriented experimental evaluation on TiC-Steel cermet with vitrified bond cBN wheel, *Ceramics International*, vol. 47, no. 24, 2021, pp. 34949-34958. https://doi.org/10.1016/j.ceramint.2021.09.036

[12] J. Dai, Y. Li, and D. Xiang, The mechanism investigation of ultrasonic roller dressing vitrified bonded CBN grinding wheel, *Ceramics International*, vol. 48, no. 17, 2022, pp. 24421-24430. https://doi.org/10.1016/j.ceramint.2022.05.049

[13] B. Zhao, W. Ding, G. Xiao, K. Cai, Z. Li, and C. Pu, Micro-fracture behavior of a single-aggregated cBN grain and its relation to material removal in high-speed grinding of Ti–6Al–4V alloys, *Journal of Manufacturing Processes*, vol. 79, 2022, pp. 19-27. https://doi.org/10.1016/j.jmapro.2022.04.052

[14] C. Zhang, S. Qu, W. Xi, Y. Liang, J. Zhao, and T. Yu, Preparation of a novel vitrified bond CBN grinding wheel and study on the grinding performance, *Ceramics International*, vol. 48, no. 11, 2022, pp. 15565-15575. https://doi.org/10.1016/j.ceramint.2022.02.090

Contribution of Individual Authors to the Creation of a Scientific Article (Ghostwriting Policy)

The authors equally contributed in the present research, at all stages from the formulation of the problem to the final findings and solution.

Sources of Funding for Research Presented in a Scientific Article or Scientific Article Itself

This research was supported by Thai Nguyen University of Technology.

Conflict of Interest

The authors have no conflicts of interest to declare that are relevant to the content of this article.

Creative Commons Attribution License 4.0 (Attribution 4.0 International, CC BY 4.0)

This article is published under the terms of the Creative Commons Attribution License 4.0
https://creativecommons.org/licenses/by/4.0/deed.en_US